

Alma Mater Studiorum – Università di Bologna

DOTTORATO DI RICERCA IN

Scienze Mediche Generali e dei Servizi - Progetto n°4:
Ultrasonologia in Medicina Umana e Veterinaria

Ciclo XXIII

Settori scientifico-disciplinari di afferenza:

Clinica Medica Veterinaria (VET/08); Medicina Interna (MED/09)

**USE OF VEGFR-2 TARGETED MICROBUBBLES
(BR55, BRACCO IMAGING) FOR THE EARLY
ULTRASOUND EVALUATION OF RESPONSE TO
ANTIANGIOGENIC TREATMENT IN A XENOGRFT
MODEL OF HEPATOCARCINOMA**

Presentata da: **BARON TOALDO dott. MARCO**

Coordinatore Dottorato

BOLONDI prof. LUIGI

Relatore

CIPONE prof. MARIO

Esame finale anno 2011

ABSTRACT

Aim: To evaluate the early response to treatment to an antiangiogenic drug (sorafenib) in a heterotopic murine model of hepatocellular carcinoma (HCC) using ultrasonographic molecular imaging.

Material and Methods: the xenograft model was established injecting a suspension of HuH7 cells subcutaneously in 19 nude mice. When tumors reached a mean diameter of 5-10 mm, they were divided in two groups (treatment and vehicle). The treatment group received sorafenib (62 mg/kg) by daily oral gavage for 14 days. Molecular imaging was performed using contrast enhanced ultrasound (CEUS), by injecting into the mouse venous circulation a suspension of VEGFR-2 targeted microbubbles (BR55, kind gift of Bracco Research, Geneva, Switzerland). Video clips were acquired for 6 minutes, then microbubbles (MBs) were destroyed by a high mechanical index (MI) impulse, and another minute was recorded to evaluate residual circulating MBs. The US protocol was repeated at day 0,+2,+4,+7, and +14 from the beginning of treatment administration. Video clips were analyzed using a dedicated software (Sonotumor, Bracco Swiss) to quantify the signal of the contrast agent. Time/intensity curves were obtained and the difference of the mean MBs signal before and after high MI impulse (Differential Targeted Enhancement-dTE) was calculated. dTE represents a numeric value in arbitrary units proportional to the amount of bound MBs. At day +14 mice were euthanized and the tumors analyzed for VEGFR-2, pERK, and CD31 tissue levels using western blot analysis.

Results: dTE values decreased from day 0 to day +14 both in treatment and vehicle groups, and they were statistically higher in vehicle group than in treatment group at day +2, at day +7, and at day +14. With respect to the degree of tumor volume increase, measured as growth percentage delta (GP Δ), treatment group was divided in two sub-groups, non-responders (GP Δ >350%), and

responders ($GP\Delta < 200\%$). In the same way vehicle group was divided in slow growth group ($GP\Delta < 400\%$), and fast growth group ($GP\Delta > 900\%$). dTE values at day 0 (immediately before treatment start) were higher in non-responders than in responders group, with statistical difference at day 2. While dTE values were higher in the fast growth group than in the slow growth group only at day 0. A significant positive correlation was found between VEGFR-2 tissue levels and dTE values, confirming that level of BR55 tissue enhancement reflects the amount of tissue VEGF receptor.

Conclusions: the present findings show that, at least in murine experimental models, CEUS with BR55 is feasible and appears to be a useful tool in the prediction of tumor growth and response to sorafenib treatment in xenograft HCC.

INTRODUCTION

Hepatocellular carcinoma (HCC) is the third leading cause of cancer death world-wide and ranks as the fifth most common cancer diagnosis globally. Unlike most malignancies, some risk factors, such as cirrhosis, viral hepatitis (e.g. hepatitis B and hepatitis C), alcohol liver disease, aflatoxin exposure, metabolic liver disease from nonalcoholic steatohepatitis (NASH), and hemochromatosis significantly increase the probability to develop HCC.¹ For these reasons, the management of HCC is strictly conditioned by the degree of liver disease and eventually by the stage of organic failure (“Child-Pugh score”).^{2,3} Recently a wide consensus in the management of HCC patients was found with the Barcelona Clinic Liver Cancer (BCLC) Staging System. Following these guidelines, patients with early HCC are candidates for curative treatments, such as surgical resection, transplantation, or local ablation via percutaneous ethanol injection or radiofrequency. Patients with intermediate HCC benefit from arterial chemoembolization, whereas patients with advanced HCC might receive antioangiogenetic drugs (Sorafenib).⁴

In a phase III randomized placebo-controlled trial, sorafenib was found to improve survival in patients with advanced-stage HCC.^{5,6} Sorafenib is a tyrosine kinase inhibitor of several intracellular proteins suspected to be important in tumor progression, including the platelet derived growth factor receptor- β (PDGFR β), *raf* kinase, and the vascular endothelial growth factor receptors (VEGFR), VEGFR-1, VEGFR-2, and VEGFR-3.¹ In preclinical studies sorafenib was found to block the RAF/MEK/ERK pathway, to inhibit tumor angiogenesis and to induce tumor cell apoptosis in HCC models.⁷

However the effects of tumor stasis and shrinkage, obtained by the administration of an antiangiogenetic drug, are usually only transitory, and, after a fleeting period of clinical benefit,

the tumor starts to grow again. In other cases no appreciable clinical effect can be obtained with the therapy, because of a total refractoriness of the tumor. Multiple mechanisms are suspected to underlie the modes of resistance to antiangiogenic treatments, through the evasions to therapies or because of a substantial indifference to the drug.^{8,9} For these reasons it is important to monitor the efficacy of the antiangiogenic therapy in order to differentiate between responders and non-responders patients, and to suspend the drug administration in those subjects who do not have benefits and might develop drug toxicity.⁶

The criteria of response to treatment used for tumor treated with conventional chemotherapy (RECIST criteria) are based on the volume reduction of the neoplasia during the drug administration.¹⁰ However antiangiogenic molecules might not induce tumor shrinkage even in presence of intra-tumoral vascular reduction and necrosis, and traditional criteria in evaluation of response to treatment might underestimate drug efficacy when these molecules are used. Considering this, a modified version of RECIST criteria, created in 2008, evaluates the response to treatment measuring the reduction in viable tumor area, assessed using contrast-enhanced radiological techniques.¹¹

The development of antiangiogenic drugs that interfere with specific pathways of vascular proliferation raised the need to find more sensitive imaging techniques in order to better assess drug efficacy and response to therapy in cancer patients. Molecular imaging refers to the characterization and measurement of biological processes at the molecular level, including techniques such as positron emission tomography, molecular magnetic resonance imaging, magnetic resonance spectroscopy, optical bioluminescence, optical fluorescence, and targeted ultrasound. However the cost and the utilization of ionizing radiations limit the use in patients of the majority of the above mentioned techniques. In contrast, ultrasound (US) is the most widely

used imaging technique, is inexpensive, portable, and provides noninvasive real-time imaging.¹²⁻

14

Ultrasound contrast agents are small, 1 to 4 micron in diameter, microbubbles (MBs) made of a gaseous core surrounded by a lipid or albumin shell. They behave hemodynamically like red blood cells, and for this reason they have the unique property to work as true intravascular tracers.^{14,15} VEGF is one of the most potent growth factors of the vascular endothelial cells. The circulating VEGF acts on some endothelium-specific tyrosine kinase receptors (VEGFR-1, VEGFR-2, VEGFR-3), that are over-expressed in tumor endothelial cells and promote vascular proliferation.^{16,17} Some VEGFR-2 targeted ultrasound contrast agents have been developed and used in experimental studies in order to monitor tumor angiogenesis and treatment efficacy.^{14,18}

BR55 (Bracco Research SA, Geneva, Switzerland) is a novel VEGFR-2 specific targeted microbubble contrast agent for the molecular imaging of angiogenesis. In contrast with other VEGFR-2 targeted MBs, BR55 does not require an antibody for binding nor uses biotin/streptavidin coupling strategy, but it contains a lipopeptide inserted in the phospholipid shell of the MB membrane. This lipopeptide is composed of a heterodimer peptide selected for its high affinity for human VEGFR-2, but that is seen to selective react also with rat vascular receptor. Because of the absence of streptavidin, highly immunogenic in human patients, BR55 is designed in view of future clinical applications.¹⁹⁻²¹

The purpose of our study is to investigate the usefulness of BR55 US contrast agent as an early predictor of response to treatment with an antiangiogenic drug (sorafenib) in a heterotopic murine model of HCC.

MATERIAL AND METHODS

Experimental model

Human cell line Huh7, kindly provided by Dr. Porretti, was maintained and expanded using standard cell culture technique in high glucose Dulbecco's Modified Eagle Medium^b supplemented with L-glutamine, 1% ampicillin/amphotericin B and 10% foetal bovine serum. The model was established by subcutaneous injection of 5×10^6 cells suspended in sterile phosphate-buffered saline^c for a total volume of 0.2 mL per injection into the right flank of 6-8 weeks old female nude mice^d. During the experiments, the mice were maintained with regular mouse chow and water *ad libitum* in a temperature-controlled room under a 12-hour light/dark cycle and specific pathogen-free circumstances. Mice were randomized to vehicle or treatment with sorafenib^a (BAY 43-9006) at a dosage of 62 mg/Kg by daily oral gavage. Sorafenib was formulated as previously described.²² Growth of established xenografts was monitored at least twice weekly by US. The treatment started when tumours reached 5-10 mm in diameter and lasted for 14 days. The protocol was approved by the Ethical Committee of the University of Bologna.

Targeted contrast enhanced ultrasound imaging

Imaging examinations were performed using an ultrasound unit^e equipped with a linear array 4-13 MHz probe. Mice were anesthetized intraperitoneally with 0.2 mL of a solution constituted by one part of ketamine^f 10%, one part of xylazine^g 20 mg/mL, and eight parts of sterile water. The anesthetized animals were placed on a heating support in order to keep constant the temperature for all the duration of the experiment. All the tumors were first visualized with Bmode ultrasonography in two perpendicular scan plains in order to measure the maximal diameters of

the mass and to calculate its volume, through the formula: height x width x thickness/2. For contrast enhanced ultrasonography (CEUS), ultrasound coupling gel was applied on the skin and the probe was placed on a fixed mechanical support in order to maintain the same scanned section of the tumor for all the duration of the US. A contrast specific software (Contrast Tune Imaging, CnTI) was activated in a dual display modality (Bmode window and contrast window). The following US setting were used and maintained unvaried for all the experiment: dynamic range, 7 dB; acoustic power, 30 kPa; mechanical index, 0.03; depth, 22-37 mm; time-gain compensation, linear.

VEGFR-2 targeted MBs contrast agent^h was reconstituted injecting 2 ml of a sterile 5% glucose solution through the septum of the vial. After dissolution of the cake, the resulting MB suspension was collected through a needle inserted through the rubber stopper. A volume of 50 μ l of MB suspension (2.4×10^7 MBs) was injected into the mouse venous circulation through the retro-orbital sinus. Immediately after the injection a video clip was acquired continuously for 6 minutes at low MI, then the MBs present into the tumor were destroyed by increasing the acoustic power (MI 1.9). Video acquisition continued for 1 minute after MBs destruction in order to evaluate residual circulating MBs during the replenishment of the tumor.

The same procedure protocol was repeated at different time points starting from the beginning of the treatment (0, +2, +4, +7 and +14 days).

Post-processing analysis of ultrasound data

Post processing analysis of US video clips, recorded as DICOM files, was performed using a dedicated softwareⁱ. This software is designed to quantify contrast echo-power within a region of interested (ROI) comprehending all the tumor area. The analysis applies first linearization at the pixel levels to revert the effects of “log” compression in the ultrasound system. Contrast

enhancement in the ROI was expressed as relative echo-power values (rms2), which are proportional to the number of MBs in the selected ROI.²¹ The software automatically recognizes the high MI flash frames, and it considers for quantifications only the 2 seconds before the flash and the 10 seconds following the 15th second after the flash. The signal intensity (defined as targeted enhancement, TE), before and after destruction (respectively TE_{bd} and TE_{ad}) were subtracted in order to obtain the differential targeted enhancement (dTE=TE_{bd}-TE_{ad}). Since the TE_{bd} is proportional to both the circulating and the bind MBs, whereas TE_{ad} corresponds only to circulating MBs that are reperfusing the tumor after high MI destruction, the difference between them (dTE) represents a numeric value proportional to the amount of bound MBs to the target receptor VEGFR-2.

Necroscopy

At day +14, after the last measurement and still under anaesthesia, animals were euthanized by intraperitoneally injection of 0.1 mL of a solution of embutramide, mebezonium iodide and tetracaine hydrochloride^j. Tumor were dissected and stored in 4% paraformaldehyde. A slice of all tumours were also frozen in liquid nitrogen vapour and stored at -80°C.

Western blot analysis

Three monoclonal antibodies (Ab) against VEGFR2^k (diluted at 1:1000), phospho-p44/42 MAPK (Erk1/2; Thr202/Tyr204)^l (diluted at 1:1000) and CD31^m (diluted at 1:1000), were incubated separately for 16 hours at 4°C. A horseradish conjugated secondary Abⁿ (diluted at 1:7500) was incubated for 45 minutes at room temperature and the corresponding band was revealed using the enhanced chemoluminescence method^o. Digital images of autoradiographies were acquired with a quantitative imaging system^p and band signals were acquired in the linear range of the scanner

using a specific densitometric software^q. Images were calibrated against a reference autoradiography and given in relative density units. After autoradiography acquisition, the membranes were stripped and reprobed for two hours at room temperature with anti β -actin antibody^r (diluted at 1:500) to normalize protein loading. A ratio between VEGFR2/phospho-ERK/CD31 and β -actin corresponding bands was used to quantify the levels of each protein (normalized value). This ratio was divided by β -actin levels of HuH7 line in each blot in order to compare the results in different running gels (absolute value).

Statistical analysis

Data are presented as median values. Differences in dTE between treated and untreated, responder and non-responder, and fast growth and slow growth tumours were compared using the Mann-Whitney test (2-tailed). Percentage delta of variation of tumour volume was calculated using the formula [(final value-starting value)/starting value]%. Data of dTE and VEGFR-2 were compared using a Spearman's rank test. A $p < 0.05$ was considered significant. Statistical analysis was performed using a dedicated software^s.

RESULTS

Tumor model and targeted ultrasound findings

A number of 19 mice (10 in the treatment group and 9 in the vehicle group) were studied from the beginning to the end of the protocol. Median tumor volume was 608.02 mm³ (333.3-1799.88) at day 14 in the treatment group and 893.43 mm³ (218.67-1996.70) in the vehicle group (Fig. 1), with a growth percentage delta of 192.76% (84.72-739.48) in treatment group and 747.56% (73.47-2887.62) in vehicle group.

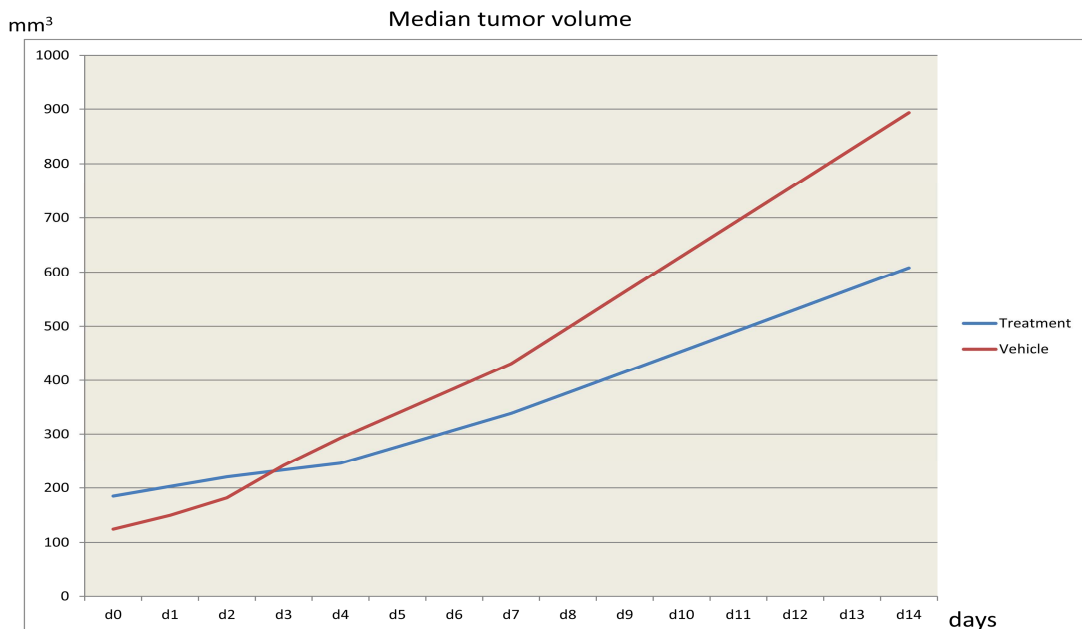


Figure 1. Median tumor volumes in treatment and vehicle group at different times from the beginning of drug administration. Median tumor volume for treatment group is 184.89 mm³ at day 0 and 608 mm³ at day 14 (growth percentage delta: 192.76%); while in vehicle group mean tumor volume is 124.61 mm³ at day 0 and 893.43 mm³ at day +14 (growth percentage delta: 747.56 %).

Median values of dTE in treated and vehicle groups at different days are listed in table 1. The lowest value for treatment group was observed at day +7, while the lowest value for vehicle

group was recorded at day +4 (Fig 2). At day +2, +7 and +14 dTE values in treatment group were consistently lower than in vehicle group (p=0.002, p=0.001 and p=0.009 respectively).

dTE	Treatment group	Vehicle Group	p value
Day 0	1,82E+07	2,94E+07	NS
Day +2	1,24E+07	2,55E+07	0.022
Day +4	3,44E+02	6,87E+06	NS
Day +7	1,21E+06	8,69E+06	0.001
Day +14	2,53E+06	1,05E+07	0.009

Table 1. dTE values (expressed as arbitrary units) for treatment and vehicle groups at different days from starting treatment-placebo administration. A significant difference between dTE in the two groups was seen at day +2, day +7, and day +14, with higher dTE values in vehicle group with respect to treatment group. A p<0.05 was considered significant.

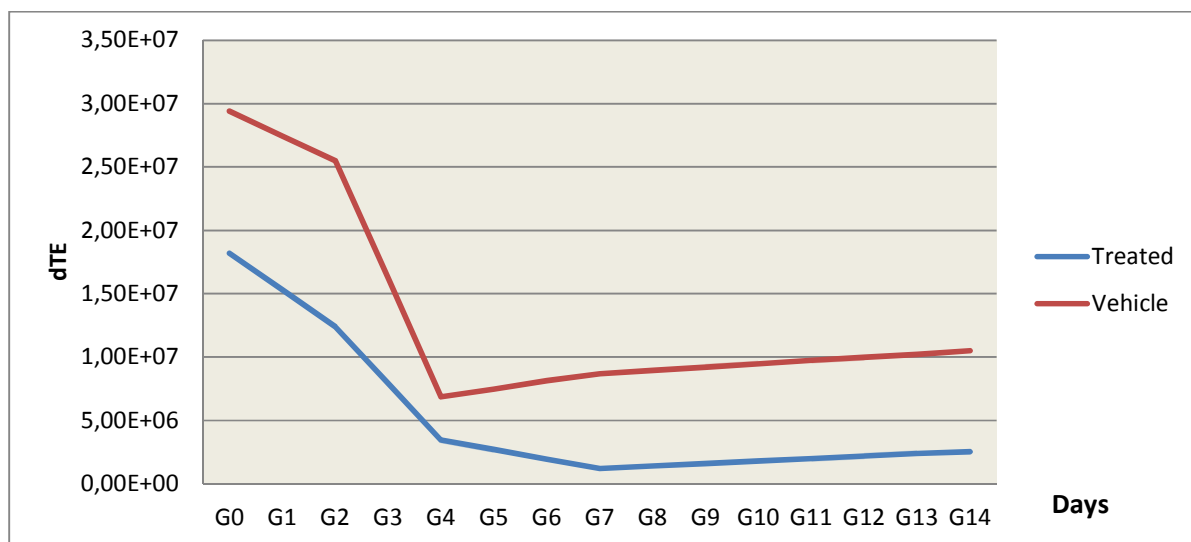


Figure 2. Median contrast enhanced derived dTE values for treatment and vehicle group at different times from the beginning of drug administration. dTE is calculated by subtracting the signal intensity from the microbubbles before and after a high mechanical index impulse. Significantly higher dTE values are reported in treatment group at day +2 (p=0.022), at day +7 (p=0.001), and at day +14 (p=0.009).

Treatment group was divided in two sub-groups with respect to growth percentage delta (GPA). Tumors with a $GPA < 200\%$ were considered as responders to treatment (6 cases, ranging from 85% to 199%). Tumors with a $GPA > 350\%$ were defined as non-responders (4 cases, ranging from 382% to 739%). Median tumor volume for responders group was $272,92 \text{ mm}^3$ at day 0 and 523.56 mm^3 at day +14. Median tumor volume for non-responders group was $107,07 \text{ mm}^3$ at day 0 and 761.69 mm^3 at day +14.

As for treatment group, vehicle group was divided in two subgroups with respect to their GPA. Tumors with slow growth had a $GPA < 400\%$ (4 mice), whilst tumor with fast growth presented a value $> 900\%$ (5 mice). Median tumor volume for slow growth group was $159,22 \text{ mm}^3$ at day 0 and $602,71 \text{ mm}^3$ at day +14. Median tumor volume for fast growth group was $105,41 \text{ mm}^3$ at day 0 and $1940,80 \text{ mm}^3$ at day +14. Figure 3 shows mean volumes for the four groups at different days.

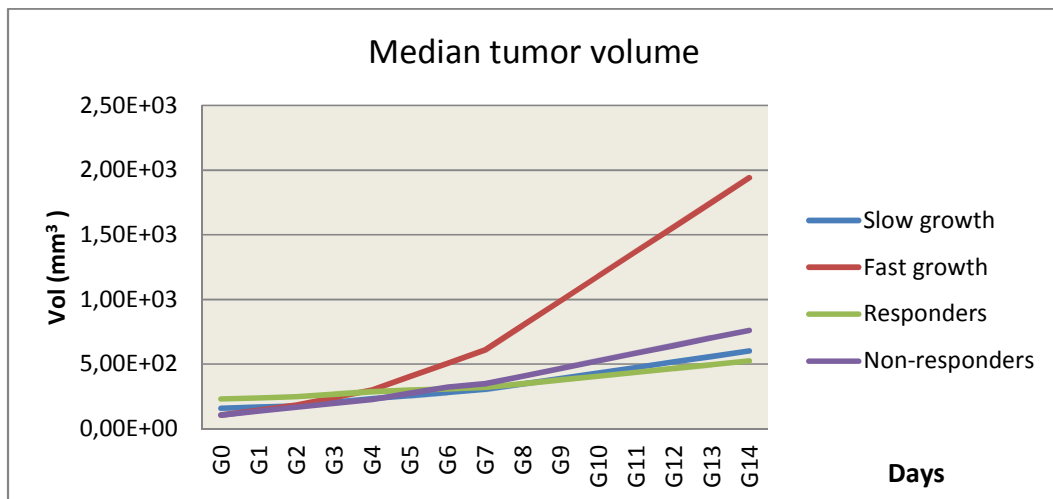


Figure 3. Median tumor volumes in the four treatment and vehicle sub-groups at different times from the beginning of drug administration. With respect to the growth percentage delta (GPA, calculated by the formula $[(\text{final value} - \text{starting value}) / \text{starting value}] \%$), treatment group is divided in responders ($GPA < 200\%$) and non-responders ($GPA > 350\%$); while vehicle group is divided in slow growth group ($GPA < 400\%$), and fast growth group ($GPA > 900\%$).

Higher values in dTE are reported for non-responders to treatment and fast growth untreated groups at day 0, while from day +4 both treatment groups present lower dTE value than the two vehicle groups (Fig. 4 and Table 2).

dTE	Non-responders	Responders	Slow growth	Fast growth
Day 0	5.92E+07	1.41E+07	1.69E+07	3.85E+07
Day 2	2.56E+07	9.22E+06	2.80E+07	2.49E+07
Day 4	5.39E+06	2.72E+06	7.72E+06	6.87E+06
Day 7	1.62E+06	9.98E+05	1.14E+07	7.79E+06
Day 14	4.39E+06	1.89E+06	1.50E+07	5.54E+06

Table 2. Median dTE values for treatment groups (non-responders and responders), and vehicle groups (slow and fast growth) at different times from the beginning of drug administration.

A significance difference in dTE values exists between responders and non-responders at day +2 (p=0.019).

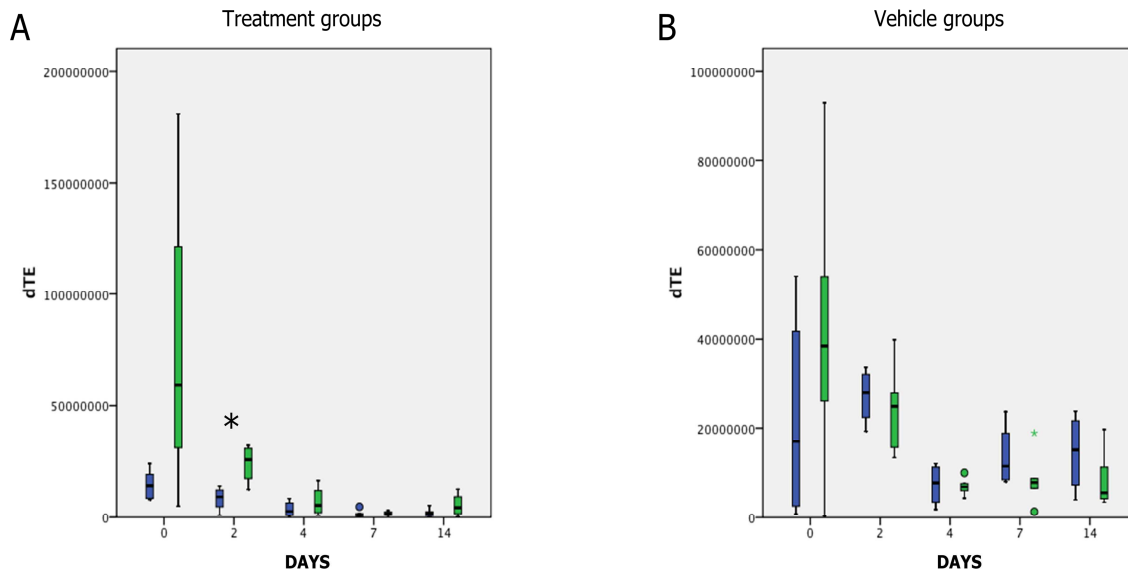


Figure 4. A. Mean dTE values and confidence intervals for treatment groups. A progressive reduction in dTE values is present for non-responders (green bars) and responders (blue bars) between day 0 and day +7, with a slight increase between day +7 and day +14. Higher values of dTE were measured for non-responders with respect to responders at all days from the beginning of drug administration. Statistical difference was present between non-responders and responders (blue bars) only at day +2 ($p=0.019$). B. Mean dTE values and confidence intervals for vehicle groups. Higher values of dTE were measured at day 0 in fast growth groups (green bars), while from day +2 to day +14 dTE values became higher in slow growth group (blue bars).

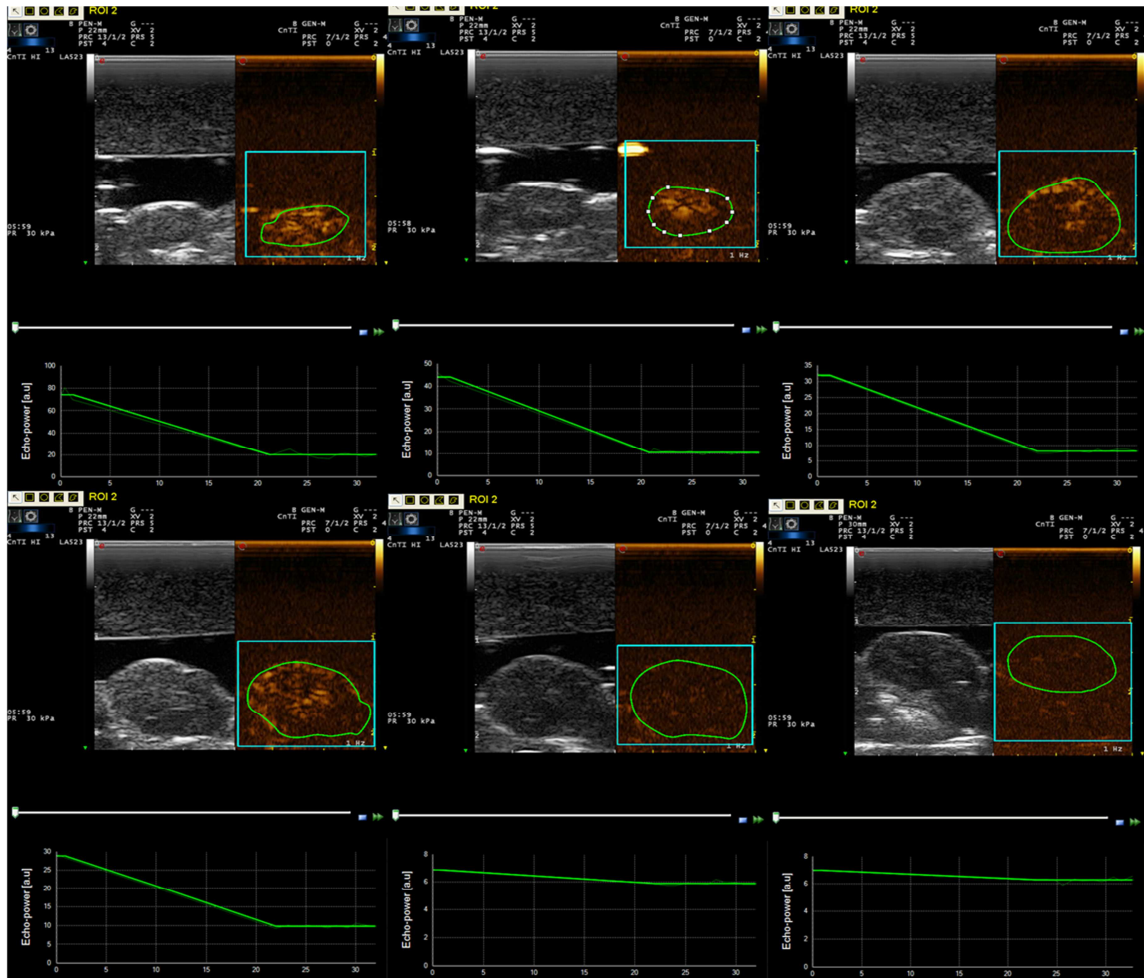


Figure 5. Contrast enhanced ultrasound images of two tumors after injection of a VEGFR-2 targeted ultrasound contrast agent (BR55). The images refer to sixth minute after injection, before the high mechanical index (MI) destruction impulse. Bound microbubbles (MBs) are represented as stationary bright colored speckles within the tumor. For quantification analysis a region of interest is drawn in order to comprehend all the tumor area. Subsequently the software automatically quantifies some frames before and after the high MI flash and it creates a time-intensity diagram with signal intensity (expressed as echo-power, measured in arbitrary units) plot in the y axis, and time (as seconds) in the x axis. The difference between the echo-power before and after MBs destruction (dTE) is proportional to the amount of MBs bound to the VEGFR-2 receptor. In the upper panel a tumor from the vehicle group is shown. A certain amount of bound MBs is visible at day 0 (left), day +2 (middle), and day +14 (right). An example of a treated tumor is shown in the lower panel. Compared with the vehicle tumor no appreciable signal is evident from bound MBs at day +2 and at day +14.

Western blot analysis

Western blot analysis for VEGFR-2, CD31 and pERK were performed for 16 tumor slices, at day +14. For technical reasons three tumors were excluded from western blot evaluation (1 from vehicle group, and 2 from treatment group). The data presented as median values and standard deviations are listed in table 3. No statistical difference was found between VEGFR-2, CD31, and pERK at day +14 between the four sub-groups (non responders and responders to treatment tumors, and slow and fast growth vehicle groups).

	Non-responders	Responders	Slow growth	Fast growth
VEGFR-2/ β -actin	4,269 (26,063-0,616)	1,043 (1,463-0,134)	0,945 (1,046-0,562)	1,781 (2,245-0,886)
VEGFR-2/ HuH7 β -actin	0,200 (01,218-0,029)	0,049 (0,068-0,006)	0,051 (00,056-0,030)	0,096 (0,121-0,048)
CD31/ β -actin	0,883 (12,523-0,354)	0,605 (2,172-0,124)	1,028 (1,525-0,172)	1,210 (2,856-0,144)
CD31/HuH7 β -actin	0,041 (0,585-0,016)	0,028 (0,102-0,006)	0,055 (0,082-0,009)	0,065 (0,153-0,008)
pERK/ β -actin	5,346 (10,646-0,570)	0,893 (1,216-0,467)	1,007 (1,401-0,612)	0,752 (2,153-0,362)
pERK/HuH7 β -actin	0,250 (0,585-0,017)	0,044 (2,172-0,124)	0,054 (0,082-0,009)	0,040 (0,116-0,019)

Table 3 Results from quantification of western blot analysis. Median and min and max (round brackets) values are expressed as arbitrary units derived from comparison between VEGFR-2, CD31, pERK levels and β -actin levels for each tumor (normalized values); absolute values were calculated considering the ratio between normalized values and HuH7 β -actin levels in order to compare data from different running blots. No statistical difference was found between western blot values in the four groups (responders and non-responders to treatment, and slow and fast growth from vehicle receiving mice). However, even in absence of statistical significance, higher values of normalized and absolute VEGFR-2 level were seen in non-responders and fast growth tumors, compared with responders and slow growth ones. Normalized and absolute values of CD31 were higher in vehicle groups and in non-responders group. pERK normalized and absolute levels were higher in non-responders and slow growth groups and slightly lower in responders and fast growth tumors.

Considering all tumors in all groups, VEGFR-2 levels expressed as absolute values ($[\text{VEGFR-2}/\beta\text{-actin}]/\text{HuH7 } \beta\text{-actin}$) were significantly related to dTE values at day +14 ($R=0.635$ and $p=0.008$).

DISCUSSION

In our study we observed that ultrasound molecular imaging using a VEGFR-2 targeted microbubble contrast agent (BR55) can be a useful tool to monitor the response to treatment to an antiangiogenic drug in a xenograft model of HCC. Signal intensity from bound MBs, measured as dTE, was statistically lower in treatment group with respect to vehicle group, very early after the beginning of drug administration (day +2), and the difference remained significant during the following days (+7, and +14). When treatment group was divided in responder and non-responders, considering the degree of volume increase, dTE were higher in non-responders subgroup at each day when compared to responders, and this was still evident at day 0, before treatment was started. However, because of the wide overlap between values, statistical difference was present only at day +2.

Sorafenib is a multiple kinase inhibitor that specifically acts on VEGFR-1, VEGFR-2, VEGFR-3, PDGFR β , and *raf* kinase and it is proved to prolong survival time in patients with advanced HCC. However the response rate to sorafenib is actually quite low (2-3%).^{1,23} The mechanism of development of resistance to antiangiogenic drugs is still not well clarified. Drug induced hypoxia may lead to induction of hypoxia-regulated factors and other pro-angiogenic factors that finally produce a rebound effect of tumor angiogenesis, with recruitment of new endothelial cells, and vascular remodeling and stability. It is known that different tumors may express different kinds of angiogenic factors, and therefore endothelial cells may exhibit a tissue type-dependent response to therapies.^{9,24} In xenograft models, in which tumor is generated by direct injection of a cell line, the endothelial cells invading the tumor derive from the mice. For this reason, the difference in response to treatment observed in our experiment, should be, at least in part, host-dependent. Monitoring anti-tumoral therapy is essential in order to identify the

occurrence of drug resistance. Dimensional criteria for evaluation of tumor response to treatment might be not suitable to monitor response to antiangiogenic therapy, because of lack of volume shrinkage even in presence of intra-tumoral vascular reduction and necrosis. Molecular imaging targeted for specific vascular pathways might be more sensitive in predicting treatment efficacy.²⁵ The expression of VEGF protein is found to correlate with clinicopathological factors such as proliferation, vascular invasion, and tumor multiplicity in HCC. Moreover VEGF expression is reported to associate not only with invasion and metastasis of HCC, but also with postoperative recurrence.¹⁶ No data are available regarding VEGFR-2 levels and tumor aggressiveness in HCC patients. However, considering the mitogenic effect of circulating VEGF ligand on vascular proliferation and VEGFR-2 overexpression in tumoral endothelial cells, targeting molecular imaging for this specific vascular receptors might be useful in recognizing more aggressive, vascularized tumors, potentially less respondent to antiangiogenic treatment.

We observed that non-responders tumors as well as fast growth ones, showed higher VEGFR-2 targeted MBs signal, measured as dTE value, before starting treatment. It can be speculated that tumors with high VEGFR-2 values present a more aggressive behavior, faster growth, and a less response to sorafenib.

BR55 is designed to bind to VEGFR-2 vascular receptor, with high affinity and specificity.^{19,21} In our experiment we observed that the amount of bound BR55 MBs is statistically related to tumoral VEGFR-2 expression, measured through western blot analysis, at day +14. We hypothesize that this correlation was present also before starting treatment at day 0, and during the follow-up period. However, further investigations are needed to confirm this observation.

A progressive reduction in dTE values was observed also in non-treated tumors between day 0 and day +4, with a slight increase between day +4 and day +14. This might be explained because of the extension of large necrotic areas secondary to rapid tumor volume increase in absence of

adequate vascular proliferation. Considering that the production of VEGF is dependent upon tumor cell mass,²⁶ the reduction of the effective vital tumoral area might be responsible of transient reduce of vascular proliferation and VEGFR-2 expression, with decreased BR55 uptake. Another possible explanation for dTE reduction in vehicle group might be attributable to a partial persistence of ligation of the lipopeptide construct of BR55 to the VEGFR-2 into the tumor. We hypothesize that after injection the bounding sub-unit of BR55 remained attached to the vascular receptor for more than a few minutes, even for some days, interfering with specific bind of new MBs, and subsequently reducing contrast uptake and finally dTE values. When the US schedule became less frequent, the lipopeptide had enough time to completely release from VEGFR-2, and dTE values started to increase, as seen between day +4 and +7, and more clearly between day +7 and +14. In vitro studies showed that BR55 MBs are displaced from VEGFR-2 by specific monoclonal Ab miming VEGF ligand. However only partial displacement occurs if low concentrations of Ab were used.¹⁹ Considering our in vivo experiment, if circulating VEGF concentrations weren't high enough to induce complete detachment of BR55, the remaining bound MB subunits might act as competitors for the new contrast agent. Further studies are needed to confirm or confute this hypothesis, in order to evaluate possible residual persistence of BR55 subunits into the tumor, even many hours after contrast agent injection.

Western blot analysis for CD31 was used to quantify vascular density in tumor slices. Lower values of CD31 were obtained for treatment group with respect to vehicle group. Moreover responders subgroup showed lower CD31 concentrations that responders tumors, and similarly slow growth subgroup had lower CD31 values than fast growth one. These data indicate that sorafenib inhibited vascular proliferation in treated compared to non-treated tumors, and that the inhibition was more efficacious in responders than non-responders and in slow growth than fast growth sub-groups.

We also analyzed pERK concentration in tumor slices through western blot. Phosphorylated ERK is the key downstream target of the RAF/MEK/ERK cascade that represents a fundamental signaling pathway involved in the regulation of normal mammalian cell proliferation, survival and differentiation. A dysregulation of this pathway is implicated in the molecular pathogenesis of HCC.²⁷⁻²⁹ In experimental studies sorafenib is seen to block the RAF/MEK/ERK pathway in a dose dependent fashion.⁷ In our study we observed that pERK expression was higher in non-responders tumors compared to responders, and to vehicle tumors. These results highlight the fact that some tumors, even if treated with sorafenib, might be refractory to drug effect, and even over-express pERK with respect to untreated HCCs. In an in vitro study Zhang and colleagues observed that baseline pre-treatment pERK was differently expressed in different HCC cell lines and that it seemed to be correlated with their metastatic potential and response to sorafenib. Cell lines with lower basal levels of pERK were significantly less sensitive to sorafenib-mediated growth inhibition than the other cell lines with higher pERK levels.²⁸ However in another in vitro study sorafenib was seen to inhibit ERK-1/2 phosphorylation at pharmacological concentrations in human bladder cancer cells, while at low concentrations sorafenib significantly stimulated ERK-1/2 phosphorylation. With respect to these data the authors concluded that sorafenib exhibits a dual (activatory and inhibitory) mode of action in a panel of human bladder cell lines.²⁹ In our experiment we used the full dose of sorafenib reported in the literature for xenograft models.²² This dose represents the therapeutic murine dose calculated from human pharmaceutical dose and we considered it high enough to produce therapeutic effect without major toxicity in the mouse.

We didn't measure pERK concentrations in tumors at baseline, before starting treatment, so we are not able to evaluate the trend of increase in ERK phosphorylation in the tumor model we used. However, the higher values in pERK observed in non-responders tumors might be

interpreted as a sorafenib induced stimulatory effect on pERK. Another possible explanation of this behavior can be found in the wide variability of response to treatment of different HCCs, with an escape to sorafenib mediated inhibitory effect and activation of other signaling pathways that act on ERK phosphorylation. Further studies are needed to elucidate this results and to evaluate the changes in pERK in different HCCs treated with sorafenib.

Conclusions

Contrast enhanced ultrasonography is a promising technique to monitor the efficacy on anti-angiogenic drugs for the treatment of hypervascularized tumors. In clinical oncology some studies reported the usefulness of non-targeted MBs for the early diagnosis of response to treatment.³⁰⁻³⁴ However molecular US might be a more specific and sensitive tool in evaluating tumor functional changes. In our study we observed that CEUS using a VEGFR-2 targeted MB contrast agent (BR55) can early predict the response to treatment with sorafenib in a xenograft model of HCC, allowing to distinguish between responders and non-responders tumors, even before starting treatment. The bounding subunit of BR55 is represented by a lipopeptide construct that is directly incorporated in the phospholipid-based microbubble shell, without the use of Ab. For these reasons, BR55 doesn't own immunogenic properties, and might be safely used in human beings. According to these observations CEUS using BR55 contrast agent might be a future useful technique for monitoring anti-tumoral therapies in clinical oncology.

Footnotes

^a Nexavar, Bayer S.p.A., Milan, Italy

^b Gibco® DMEM, Invitrogen S.r.L., San Giuliano Milanese (MI), Italy.

- ^c Gibco® Phosphate-buffered saline (10X), liquid, Invitrogen S.r.L., San Giuliano Milanese (MI), Italy.
- ^d CD1 nude, Charles River, Sant'Angelo Lodigiano (LO), Italy.
- ^e MyLab70 XVG, Esaote, Florence, Italy.
- ^f Ketavet 100, Intervet Productions S.r.l., Aprilia (LT), Italy
- ^g Rompun®, Bayer HealthCare, Milan, Italy
- ^h BR55, Bracco Swiss SA, Geneva, Switzerland
- ⁱ Sonotumor (version 4.0.4), Bracco Research SA, Geneva, Switzerland
- ^j Tanax, Intervet/Schering Plough Animal Health S.r.l., Milan, Italy
- ^k 55B11, Cell Signaling Technology, Inc. Danversa, MA, USA
- ^l 20G11, Cell Signaling Technology, Inc. Danversa, MA, USA
- ^m ab28364, Abcam, Cambridge, MA, USA
- ⁿ labeled polymer-HRP antimouse, Envision system DAKO Cytomation, Carpinteria, CA, USA
- ^o Amersham Biosciences, GE Healthcare Europe GmbH, Glattbrugg, Switzerland
- ^p Fluor-S MultiImager, Bio-Rad, Hercules, CA, USA
- ^q Quantity-one, Bio-Rad, Hercules, CA, USA
- ^r beta-Actin (C4), Santa Cruz Biotechnology, Inc. Santa Cruz, CA, USA
- ^s SPSS 16.0, SPSS Inc., Chicago, USA

References

1. Finn RS. Drug therapy: sorafenib. *Hepatology* 2010; 51(5): 1843-1849.
2. Child CG, Turcotte JG. Surgery and portal hypertension. In: The liver and portal hypertension. Philadelphia, PA: Saunders; 1964: 50-64.
3. Pugh RN, Murray-Lyon IM, Dawson JL, et al. Transection of the oesophagus for bleeding oesophageal varices. *Br J Surg* 1973; 60(8): 646-649.
4. Llovet JM, Di Bisceglie AM, Bruix J, et al. Design and endpoints of clinical trials in hepatocellular carcinoma. *J Natl Cancer Inst* 2008; 100: 698-711.
5. Llovet JM, Ricci S, Mazzaferro V, et al. SHARP Investigators. Sorafenib improves survival in advanced Hepatocellular Carcinoma (HCC): results of a phase III randomized placebo-controlled trial. *J Clin Oncol* 2007; LBA1.
6. Llovet JM, Ricci S, Mazzaferro V, et al. Sorafenib in advanced hepatocellular carcinoma. *N Engl J Med* 2008; 359: 378-390.
7. Liu L, Cao Y, Chen C, et al. Sorafenib blocks the RAF/MEK/ERK pathway, inhibits tumor angiogenesis, and induces tumor cell apoptosis in hepatocellular carcinoma model PVC/PRF/5. *Cancer Res* 2006; 66(24): 11851-11858.
8. Bergers G, Hanahan D. Modes of resistance of anti-angiogenic therapy. *Nature* 2008; 8: 592-603.
9. Cao Y, Zhong W, Sun Y. Improvement of antiangiogenic cancer therapy by understanding the mechanism of angiogenic factor interplay and drug resistance. *Seminars in Cancer Biology* 2009; 19: 338-343.
10. Therasse P, Arbuck SG, Eisenhauer EA, et al. New guidelines to evaluate the response to treatment in solid tumors. *J Natl Cancer Inst* 2000; 92(3): 205-216.

11. Lencioni R, Llovet JM. Modified RECIST (mRECIST) assessment for hepatocellular carcinoma. *Semin Liver Dis* 2010; 30: 52-60.
12. Massoud TF, Gambhir SS. Molecular imaging in living subjects: seeing fundamental biological processes in a new light. *Genes Dev* 2003; 17: 545-580.
13. Cai W, Rao J, Gambhir SS. How molecular imaging is speeding up antiangiogenic drug development. *Mol Cancer Ther* 2006; 5: 2624-2633.
14. Korpanty G, Carbon JG, Grayburn PA, et al. Monitoring response to anticancer therapy by targeting microbubbles to tumor vasculature. *Clin Cancer Res* 2007; 13(1): 323-330.
15. Deshpande N, Needles A, Willmann JK. Molecular ultrasound imaging: current status and future directions. *Clin Radiol* 2010; 65: 567-581.
16. Tanaka S, Arai S. Molecular targeted therapy for hepatocellular carcinoma. *Cancer Sci* 2009; 100: 1-8.
17. Anderson CR, Rychak JJ, Backer M, et al. scVEGF microbubble ultrasound contrast agents: a novel probe for ultrasound molecular imaging of tumor angiogenesis. *Invest Radiol* 2010; 45(10): 579-585.
18. Willmann JK, Paulmurugan R, Chen K, et al. US imaging of tumor angiogenesis with microbubbles targeted to vascular endothelial growth factor receptor type 2 in mice. *Radiology* 2008; 246(2): 508-518.
19. Pochon S, Tardy I, Bussat P, et al. BR55: a lipopeptide-based VEGFR2-targeted ultrasound contrast agent for molecular imaging of angiogenesis. *Invest Radiol* 2010; 45(2): 89-95.
20. Pysz MA, Foygel K, Rosenberg J, et al. Monitoring with molecular US and a clinically translatable contrast agent (BR55). *Radiology* 2010; 256(2): 519-527.

21. Tardy I, Pochon S, Theraulaz M, et al. Ultrasound molecular imaging of VEGFR2 in a rat prostate tumor model using BR55. *Invest Radiol* 2010; 45(10): 573-578.
22. Wilhelm SM, Carter C, Tank L, et al. BAY 43-9006 exhibits broad spectrum oral antitumor activity and targets the RAF/MEK/ERK pathway and receptor tyrosine kinase involved in tumor progression and angiogenesis. *Cancer Res* 2004; 64(19): 7099-7109.
23. Llovet JM, Ricci S, Mazzaferro V, et al. Sorafenib in advanced hepatocellular carcinoma. *N Engl J Med* 2008; 359(4): 378-390.
24. Glade Bender J, Cooney EM, Kandel JJ, et al. Vascular remodeling and clinical resistance to antiangiogenic cancer therapy. *Drug Resist Updat* 2004; 7: 289-300.
25. Lamuraglia M, Bridal SL, Santin M. Clinical relevance of contrast-enhanced ultrasound in monitoring anti-angiogenic therapy of cancer: current status and perspectives. *Crit Rev Oncol Hematol* 2010; 73: 201-212.
26. Liu Y, Poon RT, Li Q, et al. Both antiangiogenesis- and angiogenesis-independent effects are responsible for hepatocellular carcinoma growth arrest by tyrosine kinase inhibitor PTK787/ZK222584. *Cancer Res* 2005; 65(9): 3691-3699.
27. Dhillon AS, Hagan S, Rath O, et al. MAP kinase signaling pathways in cancer. *Oncogene* 2007; 26: 3279-3290.
28. Zhang Z, Zhou X, Shen H, et al. Phosphorylated ERK is a potential predictor of sensitivity to sorafenib when treating hepatocellular carcinoma: evidence from an in vitro study. *BMC Med* 2009; 7: 41.
29. Rose A, Grandoch M, vom Dorp F, et al. Stimulatory effects of the multi-kinase inhibitor sorafenib on human bladder cancer cells. *Br J Pharmacol* 2010; 160: 1690-1698

30. De Giorgi U, Aliberti C, Benea G, et al. Effect of angiosonography to monitor response during imatinib treatment in patients with metastatic gastrointestinal stromal tumors. *Clin Cancer Res* 2005; 11(17): 6171-6176.
31. Lamuraglia M, Escudier B, Chami L, et al. To predict progression-free survival and overall survival in metastatic renal cancer treated with sorafenib: Pilot study using dynamic contrast-enhanced Doppler ultrasound. *Eur J Cancer* 2006; 42(15): 2472-2479.
32. Lassau N, Lamuraglia M, Vanel D, et al. Doppler US with perfusion software and contrast medium injection in the early evaluation of isolated limb perfusion of limb sarcomas: prospective study of 49 cases. *Ann Oncol* 2005; 16(7): 1054-1060.
33. Hochedez P, Lassau N, Bonvalot S, et al. Treatment of local recurrent melanomas by isolated limb perfusion: value of Doppler ultrasonography. *J Radiol* 2003; 84(5): 597-603.
34. Lassau N, Lamuraglia M, Chami L, et al. Gastrointestinal stromal tumors treated with imatinib: monitoring response with contrast-enhanced sonography. *Am J Roentgenol* 2006; 187(5): 1267-1273.